3-2010

Ultra-thin ultra-smooth and low-loss silver films on a germanium wetting layer

Weiqiang Chen
Purdue University - Main Campus, wqchen@umich.edu

Mark D. Thoreson
Purdue University - Main Campus, mthoreso@purdue.edu

Satoshi Ishii
Purdue University - Main Campus, sishii@purdue.edu

Alexander V. Kildishev
Birck Nanotechnology Center, School of ECE, kildishev@purdue.edu

V. M. Shalaev
Birck Nanotechnology Center and School of Electrical and Computer Engineering, *Purdue University*, shalaev@purdue.edu

Chen, Weiqiang; Thoreson, Mark D.; Ishii, Satoshi; Kildishev, Alexander V.; and Shalaev, V. M., "Ultra-thin ultra-smooth and low-loss silver films on a germanium wetting layer" (2010). *Birck and NCN Publications.* Paper 698.
http://dx.doi.org/10.1364/OE.18.005124

Ultra-thin ultra-smooth and low-loss silver films on a germanium wetting layer

Weiqiang Chen, Mark D. Thoreson, Satoshi Ishii, Alexander V. Kildishev and Vladimir M. Shalaev*

Birck Nanotechnology Center and School of Electrical and Computer Engineering, Purdue University, West Lafayette, IN 47907, USA
**shalaev@purdue.edu*

Abstract: We demonstrate a method to fabricate ultra-thin, ultra-smooth and low-loss silver (Ag) films using a very thin germanium (Ge) layer as a wetting material and a rapid post-annealing treatment. The addition of a Ge wetting layer greatly reduces the surface roughness of Ag films deposited on a glass substrate by electron-beam evaporation. The percolation threshold of Ag films and the minimal thickness of a uniformly continuous Ag film were significantly reduced using a Ge wetting layer in the fabrication. A rapid post-annealing treatment is demonstrated to reduce the loss of the ultra-thin Ag film to the ideal values allowed by the quantum size effect in smaller grains. Using the same wetting method, we have also extended our studies to ultra-smooth silver-silica lamellar composite films with ultra-thin Ag sublayers.

OCIS codes: (160.3900) Metals; (240.0310) Thin films; (310.3840) Materials and process characterization; (310.6860) Thin films, optical properties.

References and links

1. J. B. Pendry, "Negative refraction makes a perfect lens," Phys. Rev. Lett. **85**(18), 3966–3969 (2000).
2. S. A. Ramakrishna, J. B. Pendry, M. C. K. Wiltshire, and W. J. Stewart, "Imaging the near field," J. Mod. Opt. **50**, 1419–1430 (2003).
3. N. Fang, H. Lee, C. Sun, and X. Zhang, "Sub-diffraction-limited optical imaging with a silver superlens," Science **308**(5721), 534–537 (2005).
4. D. O. S. Melville, R. J. Blaikie, and C. R. Wolf, "Submicron imaging with a planar silver lens," Appl. Phys. Lett. **84**(22), 4403–4405 (2004).
5. D. O. S. Melville, and R. J. Blaikie, "Super-resolution imaging through a planar silver layer," Opt. Express **13**(6), 2127–2134 (2005).
6. P. Chaturvedi, W. Wu, V. J. Logeeswaran, Z. Yu, M. S. Islam, S. Y. Wang, R. S. Williams, and N. Fang, "Molecular Scale Imaging with a Smooth Superlens" (2009) *http://arxiv.org/abs/0906.1213*.
7. H. Lee, Y. Xiong, N. Fang, W. Srituravanich, S. Durant, M. Ambati, C. Sun, and X. Zhang, "Realization of optical superlens imaging below the diffraction limit," N. J. Phys. **7**, 255 (2005).
8. Y. Xiong, Z. Liu, C. Sun, and X. Zhang, "Two-dimensional Imaging by far-field superlens at visible wavelengths," Nano Lett. **7**(11), 3360–3365 (2007).
9. Z. W. Liu, H. Lee, Y. Xiong, C. Sun, and X. Zhang, "Far-field optical hyperlens magnifying sub-diffraction-limited objects," Science **315**(5819), 1686–1686 (2007).
10. Z. Jacob, L. V. Alekseyev, and E. Narimanov, "Semiclassical theory of the hyperlens," J. Opt. Soc. Am. A **24**(10), A52–A61 (2007).
11. A. V. Kildishev, and V. M. Shalaev, "Engineering space for light via transformation optics," Opt. Lett. **33**(1), 43–45 (2008).
12. A. V. Kildishev, U. K. Chettiar, Z. Jacob, V. M. Shalaev, and E. E. Narimanov, "Materializing a binary hyperlens design," Appl. Phys. Lett. **94**(7), 071102 (2009).
13. Y. Xiong, Z. W. Liu, and X. Zhang, "A simple design of flat hyperlens for lithography and imaging with half-pitch resolution down to 20 nm," Appl. Phys. Lett. **94**(20), 203108 (2009).
14. X. Zhang, and Z. W. Liu, "Superlenses to overcome the diffraction limit," Nat. Mater. **7**(6), 435–441 (2008).
15. A. V. Kildishev, and E. E. Narimanov, "Impedance-matched hyperlens," Opt. Lett. **32**(23), 3432–3434 (2007).
16. A. Salandrino, and N. Engheta, "Far-field subdiffraction optical microscopy using metamaterial crystals: Theory and simulations," Phys. Rev. B **74**(7), 075103 (2006).
17. I. I. Smolyaninov, Y. J. Hung, and C. C. Davis, "Magnifying superlens in the visible frequency range," Science **315**(5819), 1699–1701 (2007).
18. P. B. Johnson, and R. W. Christy, "Optical-Constants of Noble-Metals," Phys. Rev. B **6**(12), 4370–4379 (1972).

#120778 - $15.00 USD Received 1 Dec 2009; revised 24 Dec 2009; accepted 5 Jan 2010; published 25 Feb 2010

19. V. P. Drachev, U. K. Chettiar, A. V. Kildishev, H. K. Yuan, W. S. Cai, and V. M. Shalaev, "The Ag dielectric function in plasmonic metamaterials," Opt. Express **16**(2), 1186–1195 (2008).
20. L. Vj, N. P. Kobayashi, M. S. Islam, W. Wu, P. Chaturvedi, N. X. Fang, S. Y. Wang, and R. S. Williams, "Ultrasmooth Silver Thin Films Deposited with a Germanium Nucleation Layer," Nano Lett. **9**(1), 178–182 (2009).
21. V. Shalaev, *Optical properties of nanostructured random media* (Springer, Berlin, 2002).
22. P. Nyga, V. P. Drachev, M. D. Thoreson, and V. M. Shalaev, "Mid-IR plasmonics and photomodification with Ag films," Appl. Phys. B **93**(1), 59–68 (2008).
23. K. Seal, M. A. Nelson, Z. C. Ying, D. A. Genov, A. K. Sarychev, and V. M. Shalaev, "Growth, morphology, and optical and electrical properties of semicontinuous metallic films," Phys. Rev. B **67**(3), 035318 (2003).
24. A. Sarychev, and V. Shalaev, *Electrodynamics of metamaterials* (World Scientific, Singapore, 2007).
25. V. M. Shalaev, and M. I. Stockman, "Fractals - Optical Susceptibility and Giant Raman-Scattering," Z. Phys. D At. Mol. Clust. **10**(1), 71–79 (1988).
26. V. A. Podolskiy, A. K. Sarychev, E. E. Narimanov, and V. M. Shalaev, "Resonant light interaction with plasmonic nanowire systems," J. Opt. A: Pure and Appl. Opt. special issue on Metamaterials (Amst.) **7**, S32–S37 (2005).
27. H. Lüth, *Solid surfaces, interfaces and thin films* (Springer, New York, NY, 2001).
28. J. Israelachvili, *Intermolecular and surface forces* (Academic press, London, 1992).
29. K. Kendall, "Solid-Surface Energy Measured Electrically," J. Phys. D Appl. Phys. **23**(10), 1329–1331 (1990).
30. R. J. Jaccodine, "Surface Energy of Germanium and Silicon," J. Electrochem. Soc. **110**(6), 524–527 (1963).
31. D. R. Lide, "CRC Handbook of Chemistry and Physics," (CRC Press, Boca Raton, FL, 2008).
32. X. Ni, Z. Liu, and A. V. Kildishev, "PhotonicsDB: Optical Constants" (2007), DOI:10254/nanohub-r3692.5.
33. S. Ishii, U. K. Chettiar, X. Ni, and A. V. Kildishev, "PhotonicsRT: Wave Propagation in Multilayer Structures" (2008), DOI:10254/nanohub-r5968.8.
34. A. Pinchuk, U. Kreibig, and A. Hilger, "Optical properties of metallic nanoparticles: influence of interface effects and interband transitions," Surf. Sci. **557**(1-3), 269–280 (2004).
35. A. Hilger, M. Tenfelde, and U. Kreibig, "Silver nanoparticles deposited on dielectric surfaces," Appl. Phys. B **73**(4), 361–372 (2001).

1. Introduction

Plasmonic materials are used in a variety of devices and are especially important in the recent boom of metamaterials. Two applications of plasmonic materials, the near-field superlens [1–7] and the far-field hyperlens [8–17], have attracted a great deal of both theoretical and experimental research interest, with recent work showing very exciting sub-diffraction resolution results [2–9] from such devices. Silver (Ag) is the most-often used metal material in superlens and hyperlens applications due to the fact that Ag exhibits the lowest on-resonance loss of any natural noble metal at optical frequencies [18, 19]. The qualities of a silver film superlens, such as film roughness and thickness, are vital to the achievable imaging resolution, and sub-diffraction resolution requires a smooth and thin metal film from the fabrication process [6, 7].

Near-field superlensing occurs when the real part of the complex, frequency-dependent superlens permittivity $\varepsilon_{SL}(\omega) = \varepsilon_{SL}'(\omega) + i\varepsilon_{SL}''(\omega)$ satisfies the condition $\varepsilon_{SL}'(\omega) = -\varepsilon_H'(\omega)$, where $\varepsilon_H'(\omega)$ is the real part of the host material's complex permittivity. Pure-silver superlenses [2] have the drawback that they cannot be very thick due to the loss in Ag, which typically limit the film thickness to 25-35 nm. Planar multi-layer (lamellar) composite materials could be used in place of pure silver in order to transfer images at larger distances [2]. In addition to planar lamellar superlens designs, the recent advanced theories and proof-of-concept experimental studies of hyperlens-based devices [9–12, 15, 17]. These hyperlens devices, including a magnifying planar hyperlenses and light concentrators [11], have provided us with a new perspective on magnifying subwavelength imaging using structures made of curvilinear, lamellar, metal-dielectric nanocomposite materials. All of the hyperlens-based designs and experiments mentioned above employ curvilinear, binary, metal-dielectric composites, i.e. lamellar structures made of two distinct materials with non-uniform layer thicknesses. A schematic example of a binary, lamellar structure is shown in Fig. 1, where a curvilinear, layered structure is deposited on top of a substrate with a 2D bump. In general, the curvilinear Ag-layers have spatially-dependent thicknesses and may have different minimal thicknesses in different layers. In addition, the desired minimal thickness quite often goes beyond the typical thickness values (20 nm) for Ag films fabricated without wetting, causing great difficulty in the successful fabrication of hyperlens-based devices.

#120778 - $15.00 USD Received 1 Dec 2009; revised 24 Dec 2009; accepted 5 Jan 2010; published 25 Feb 2010

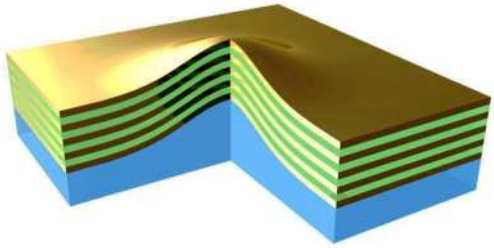

Fig. 1. Schematic of a curvilinear lamellar metal-dielectric structure for hyperlens applications.

A further hurdle in superlens and hyperlens fabrication is that the required lamellar nanocomposites often exhibit high surface roughness, which limits their overall imaging capabilities by decreasing the ultimate resolution that can be achieved with the superlens and the overall performance of hyperlens-type devices. Even with pure-metal superlenses, surface roughness limitations are problematic [2, 6], but hyperlens-type devices put forth even more demanding constraints on surface roughness in addition to the stringent requirements for control over the non-uniform thickness of individual curvilinear layers and most importantly over the minimal thickness of the continuous metal film. The realization of an advanced effective medium theory (EMT) developed for example for circular hyperlenses [12] indicates that substantial performance improvement can be achieved provided that ultra-thin, continuous Ag films are readily available.

Recent work has shown promise in using a germanium (Ge) wetting layer during the fabrication process to reduce the surface roughness of an Ag film [6, 20]. In this work, we have extended these studies and investigated the possibility of reducing the roughness of a composite superlens design through the addition of a wetting layer. To address both superlens and hyperlens demands, we specifically examined the effects of adding a Ge wetting layer on (a) the percolation threshold of ultra-thin Ag films and (b) the roughness and optical properties of ultra-thin Ag films and silver-silica nanocomposite films. A rapid post-annealing method was also explored for reducing the loss of the ultra-thin Ag films.

2. Experiment

2.1 Fabrication

Silver films were fabricated on Ge/SiO_2/glass or Ge/SiO_2/Si substrates to study the wetting effect of the thin Ge layer. All of the samples were fabricated using an electron-beam evaporation system (CHA Industries Model 600); the layers were deposited sequentially on the initial glass and Si wafer substrates without breaking the chamber vacuum. The evaporation chamber base pressure was about 1.3×10^{-4} Pa (1×10^{-6} Torr), and the evaporation rates were 0.05nm/s for Ag and Ge and 0.1 nm/s for SiO_2. Deposition rates were monitored in real time with a quartz crystal oscillator, and hence all quoted layer thicknesses herein are actually mass average thicknesses. The initial glass and silicon substrates were cleaned using several steps, including multiple solvent rinses, a piranha (H_2O_2:$3H_2SO_4$) acid bath, several ultrapure water rinses and drying with pressurized gaseous nitrogen. Silver (99.9999%, Alfa Aesar), germanium (99.999%, Cerac) and SiO_2 (99.995%, Kurt J. Lesker Corp.) source materials were used to fabricate the samples. The samples fabricated on glass substrates were used for far-field spectral measurements, while those fabricated on silicon wafers were used for high-resolution SEM imaging. We first deposited 10 nm of SiO_2 on the substrate for the purpose of eliminating the influence of the substrate roughness on the results. Next, a 1-nm Ge layer was deposited as a wetting layer. Finally, a Ag layer was deposited on the Ge/SiO_2 layers.

2.2 Percolation threshold of silver films

First, the influence of a thin Ge wetting layer on the Ag percolation threshold has been studied through the optical spectrum. During the deposition of a Ag layer on glass or

#120778 - $15.00 USD Received 1 Dec 2009; revised 24 Dec 2009; accepted 5 Jan 2010; published 25 Feb 2010

amorphous SiO_2, the deposited Ag gradually changes from a film consisting of isolated particles and clusters to a conducting film with an "infinite" metal cluster spanning over the whole sample as the metal thickness increases. This transition point between the two regimes (insulating and conducting) is called the percolation threshold [21–24]. At the percolation threshold, a strong wing in the long-wavelength part of the absorption spectrum of the Ag film appears and is associated with "hot spots" in the film [21–25], so that the spectral response of the film can be used to indicate the threshold, as we describe below.

In order to find the percolation threshold of Ag on SiO_2 with a 1-nm Ge wetting layer, a group of samples were fabricated with Ag layer thicknesses varying from 1 nm to 8.5 nm. The fabrication parameters and root-mean-squared (RMS) surface roughness values of these samples are shown in Table 1. The far-field spectral responses (transmittance and reflectance) of the samples were measured by a PerkinElmer Lambda 950 UV-Vis-NIR spectrophotometer with an integrating sphere accessory; the measured results are shown in Fig. 2. Note that that the features in the spectra near 860 nm are artifacts in our measurement setup and are not features of the sample response.

Table 1. Ag films with varying thicknesses

Sample number	**#1**	**#2**	**#3**	**#4**	**#5**	**#6**
Ag thickness (nm)	1	1.5	3	5	6.5	8.5
RMS roughness (nm)	0.22	0.295	0.489	0.287	0.596	0.73

At the beginning of the deposition process, the metal forms small, isolated particles and their clusters on the substrate. Such a film (Sample #1, 1 nm Ag) shows strong absorbance near the plasmon resonance wavelength of single particles and small clusters [21] and high transmittance for longer wavelengths. With the deposition of more metal, the metal starts to form clusters of particles with complicated morphologies. These elongated islands [26] and clusters of metal resonate in a broad spectral range, extending from the UV into the near-IR and beyond [21, 22]. As a result, the absorption spectrum of the film broadens toward the long-wavelength range.

At a particular point in the deposition process, the isolated metallic clusters connect together, and a conductive path of metal is created between the ends of the film [21, 22]. This point is known as the percolation threshold, and at this point the semicontinuous metal film changes its character from predominantly dielectric to metallic (conducting) in nature [21–24]. At the percolation threshold (Sample #3, 3 nm Ag), the transmittance (T), reflectance (R) and absorbance (A) of the film are almost independent of wavelength beyond the bulk-metal plasma resonance [21–24]. The T, R and A spectral curves tend to broaden and flatten near the percolation threshold, showing a broadband and strong absorbance response for the film.

As still more metal is deposited beyond the percolation threshold (Samples #3-6, 3-8.5 nm Ag), the additional metal tends to fill in the voids between the islands, eventually producing a uniform and completely continuous Ag film that is strongly reflective. In this regime (above percolation), the absorbance gradually decreases with increasing metal deposition in a wide wavelength range due to the loss of structures resonant at those wavelengths. For Ag films that are only slightly above the percolation threshold (Samples #3-4, 3-5 nm Ag), a large number of dielectric voids exist in the films, and the absorbance can be still relatively strong in a wide wavelength range. The long-wavelength-resonant plasmon modes in the film gradually disappear as the number of voids and the coupling between voids decreases with additional deposited metal. At this point the film finally becomes completely continuous (Samples #5-6, 6.5-8.5 nm Ag).

#120778 - $15.00 USD Received 1 Dec 2009; revised 24 Dec 2009; accepted 5 Jan 2010; published 25 Feb 2010

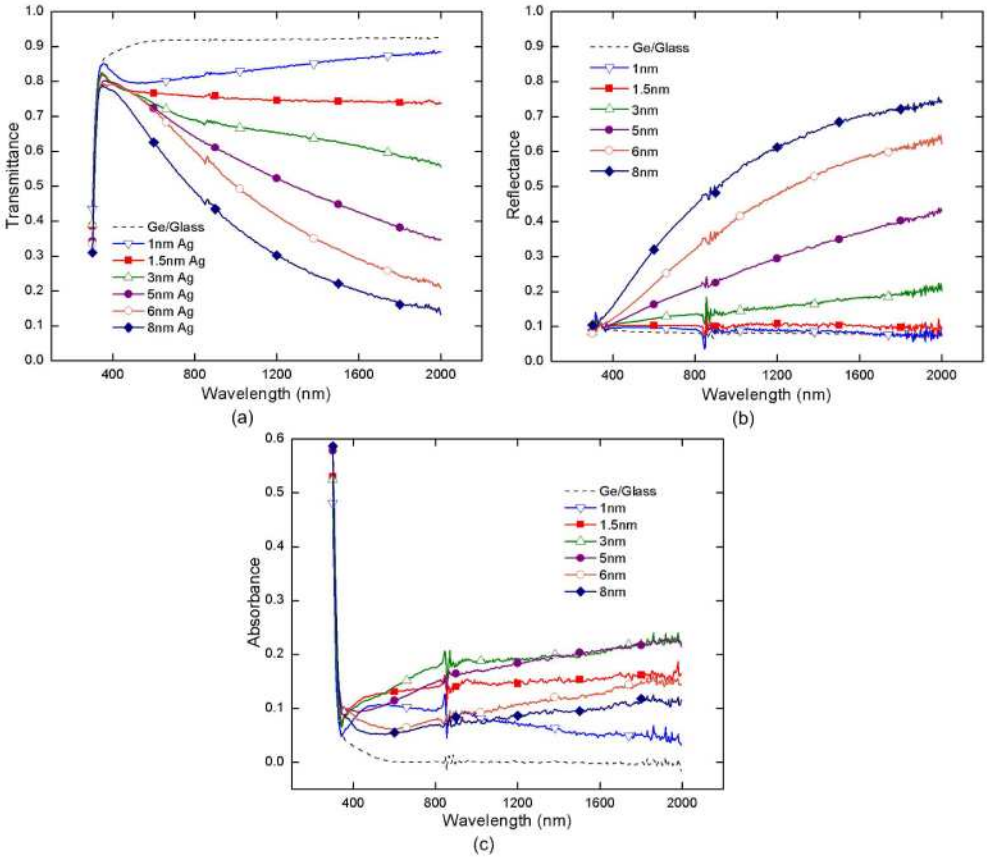

Fig. 2. Far-field spectra of Ag films with varying thicknesses deposited on SiO_2 with a 1-nm Ge layer. (a) transmittance, (b) reflectance and (c) absorbance. The percolation threshold is estimated to occur around a Ag thickness of 3 nm.

Using the results in Fig. 2, we estimate the percolation threshold of Ag deposited on a 1-nm Ge layer to be about 3 nm, which is much thinner than the 11 nm percolation threshold typically observed for e-beam deposition of Ag on SiO_2 [22]. A continuous Ag film can also be obtained at a much lower film thickness when using Ge as a wetting material. Typically an Ag film thicker than 5.5 nm is already uniformly continuous on a Ge wetting layer in our experiments, while without the Ge layer a continuous film occurs at a thickness around 20 nm.

Figure 3 shows representative SEM images of Ag films with a Ge wetting layer (Fig. 3(a)) and without the wetting layer (Fig. 3(b)). Note that these samples were fabricated on a Si(100) wafer under the same conditions as those mentioned above for the samples with glass substrates. Figure 3(a) shows a typical SEM image of 6-nm-thick Ag film on a Ge wetting layer. The SEM image was obtained at the edge of a shadowed, uncoated region to show more clearly that the film is indeed continuous. The light gray area in upper left region of the image is the Ag continuous film, while the black area is the bare Si substrate. In comparison, Fig. 3(b) shows a typical SEM image of a 6-nm-thick Ag film on a SiO_2/Si(100) substrate. Without the Ge wetting layer, the 6-nm-thick Ag film clearly consists of isolated irregular islands of metal on the substrate.

#120778 - $15.00 USD Received 1 Dec 2009; revised 24 Dec 2009; accepted 5 Jan 2010; published 25 Feb 2010

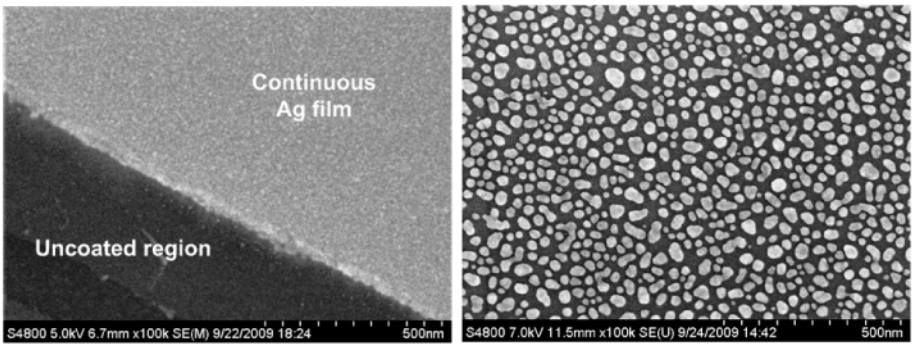

Fig. 3. Comparison between a Ag layer with and without a Ge wetting layer. (a) SEM image of 6-nm-thick Ag continuous film on a Ge/SiO_2/Si(100) substrate. The light-gray area in the image is the Ag continuous film, and the black area is an uncoated region of the Si substrate. (b) SEM image of 6-nm-thick Ag film fabricated in the same way but without the Ge wetting layer. The film consists of isolated islands of metal.

2.3 Surface roughness

The surface roughness of a metal film is a vital factor for optical applications such as superlenses and hyperlenses. Recently published experimental results have shown that when the root-mean-squared (RMS) roughness of a Ag film is higher than 1 nm, the resolution of a superlens is drastically reduced [6, 7]. Seeking to combat this resolution degradation, Logeeswaran *et al.* recently reported that a thin Ge layer can reduce the surface roughness of a 20-nm continuous Ag film [20]. Our studies show that this phenomenon is actually effective for both semicontinuous and continuous Ag films.

In order to characterize the surface morphologies of our samples and determine the effect of a Ge sublayer on the final film roughness, we performed extensive atomic force microscope (AFM) studies of the prepared samples. The surface morphologies were observed at room temperature using a Veeco Dimension 3100 AFM in a non-contact, tapping mode with a scan size of 1 μm × 1 μm, a scan rate of 1 Hz and standard Si tapping mode tips. The collected AFM topographs were characterized by computing the RMS roughness values of each sample. The RMS roughness values of Ag films with a Ge layer (Samples #1-6) varied from 0.22 nm to 0.73 nm, as listed in Table 1. Without the Ge wetting layer, however, the RMS roughness values of Ag films were typically above 2 nm in our experiments. This result confirms that the addition of a Ge wetting layer strongly reduces the surface roughness of continuous Ag films. In addition, our results indicate for the first time that a Ge wetting layer has a similar roughness-reducing effect on semicontinuous Ag films.

We extended these roughness studies to see if the technique is also effective for $(Ag/Ge/SiO_2)_n$ lamellar composite films. These films consist of n sets of Ag/Ge/SiO_2 composite layers. A (10nm Ag/1nm Ge/10nm $SiO_2)_3$ sample was prepared on a glass substrate using the same e-beam deposition methods mentioned above. The sample was fabricated by sequentially depositing a 10-nm SiO_2 layer followed by a 1-nm Ge wetting layer and a 10-nm Ag layer and then repeating this process three times to produce the final multilayer (lamellar) sample. The surface morphology of this lamellar composite sample was also studied by AFM techniques. A typical AFM topography from the sample is shown in Fig. 4. The RMS roughness of the lamellar composite film is only about 0.42 nm, which is close to that of a single-layer Ag film on a Ge wetting layer. Hence, it can be concluded that the inclusion of a Ge wetting layer below every Ag layer in the lamellar composite structure can significantly improve the final surface roughness of a multilayer, lamellar sample.

#120778 - $15.00 USD Received 1 Dec 2009; revised 24 Dec 2009; accepted 5 Jan 2010; published 25 Feb 2010

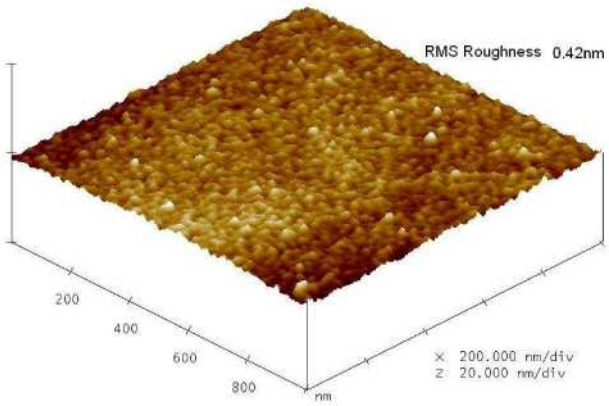

Fig. 4. Representative AFM topograph of a lamellar (10nm Ag/1nm Ge/10nm SiO_2)$_3$/glass sample. The RMS roughness is 0.42 nm, which is comparable to that of a single-layer Ag sample deposited on a thin Ge layer.

2.4 Mechanism of the wetting effect

Our fabrication results show that the growth of Ag on amorphous Ge follows the Volmer-Weber (island) growth model, although according to Ref [27]. the growth of Ag on single-crystal Ge follows the Stranski-Krastanov (layer-plus-island) growth model. Due to its relatively high surface energy, however, amorphous Ge still produces a good wetting effect for the Ag growth, since a deposited film tends to wet on a high energy surface [28]. The representative surface energies of Ag, Ge and SiO_2 are about 1.2-1.42 J/m^2, 1.06-1.835 J/m^2 and 0.26 J/m^2, respectively [29, 30]. Germanium has a higher surface energy than that of either Ag or SiO_2, meaning that the Ag atom clusters deposited on a Ge surface tend to be flatter than the same clusters deposited on SiO_2. As a result, an Ag film on Ge is smoother and exhibits a lower percolation threshold than a Ag film on SiO_2, as has been observed in our experiments. This phenomenon can also be described in terms of bond dissociation energies (enthalpy) of Ag-Ag and Ag-Ge, which are 162.9±2.9 kJ/mol and 174.5±21 kJ/mol, respectively [31]. The higher Ag-Ge bond energy (as compared to the Ag-Ag bond energy) indicates that the Ag atoms tend to be more tightly bound to the Ge surface than they are to their neighboring Ag atoms, which is a situation that is not prevalent in Ag-SiO_2 interfaces. Hence Ag islands on a Ge layer tend to be flatter (smoother) than Ag islands on SiO_2.

3. Simulations

In order to further understand our experimental results, the spectral responses and permittivities of the Ag films and the lamellar composite films were simulated using the Drude-Lorentz model for Ag with five Lorentz oscillators [18, 19, 32, 33], as shown in Eq. (1),

$$\varepsilon = \varepsilon_1 - \frac{\omega_p^2}{\omega^2 + i\gamma_p\omega} + \sum_{m=1}^{5} \frac{f_m\omega_m^2}{\omega_m^2 - \omega^2 - i\gamma_m\omega}, \qquad (1)$$

where ε_1 = 2.1485, ω_p = 9.1821 eV, ω_1 = 4.180 eV, f_1 = 0.1227, γ_1 = 0.2659 eV, ω_2 = 4.5309 eV, f_2 = 0.2167, γ_2 = 0.4269 eV, ω_3 = 5.0094 eV, f_3 = 0.2925, γ_3 = 0.6929 eV, ω_4 = 5.7530 eV, f_4 = 0.4305, γ_4 = 1.1210 eV, ω_5 = 6.9104 eV, f_5 = 0.6943, γ_5 = 1.3410 eV, and damping rate γ_p = 0.0210 eV, when fitting to the Johnson & Christy bulk silver results [18]. For our thinner films, γ_p = 0.13 eV (8.5 nm Ag), γ_p = 0.19 eV (6.5 nm Ag), γ_p = 0.21 eV (5.5 nm Ag), and γ_p = 0.2 eV (Ag in the lamellar composite films). The increased damping rates for thinner films can be explained by electron scattering at the metal boundaries [19, 34, 35] (see also below).

The Ge layer and the glass substrate were also included in the simulations to match the experimental results [32, 33]. The measured and simulated spectral results for continuous Ag

#120778 - $15.00 USD Received 1 Dec 2009; revised 24 Dec 2009; accepted 5 Jan 2010; published 25 Feb 2010

films with thicknesses ranging from 5.5 nm to 8.5 nm are shown in Fig. 5. The simulated results match our experimental results quite well in the wavelength range of interest (near-ultraviolet to near-infrared). This indicates that the Drude-Lorentz model provides a reasonable approximation of the frequency-dependent permittivity of our samples for the films that are well beyond the percolation threshold and are uniformly continuous. Note that Ag films thinner than 5 nm are not continuous and are characterized by irregularly shaped metal clusters that cannot be described by the Drude-Lorentz model alone; in this case the spectra strongly depend on the metal filling factor [21, 22].

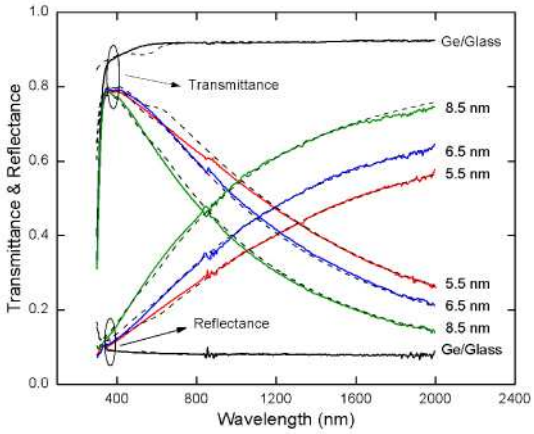

Fig. 5. Comparison of measured and simulated transmittance and reflectance spectra for Ag films beyond the percolation threshold deposited on Ge wetting layers. The solid lines represent the experimental results, and dashed lines are the simulated results.

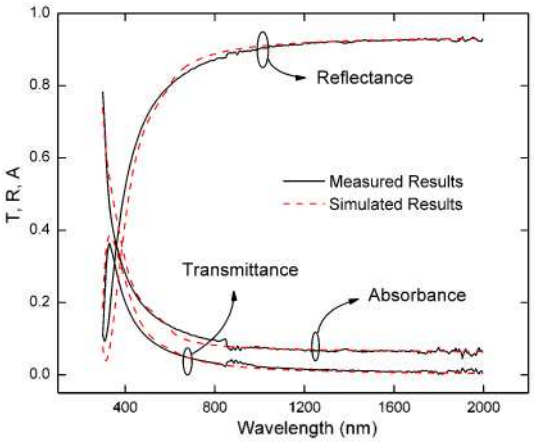

Fig. 6. Comparison of measured and simulated transmittance, reflectance and absorbance spectra for a (10nm Ag/1nm Ge/10nm $SiO_2)_3$ lamellar composite film. The solid lines represent the experimental results, while the dashed lines are the simulation results.

Figure 6 shows the measured and simulated spectral results of the (10nm Ag/1nm Ge/10nm $SiO_2)_3$ lamellar composite film. The measured and simulated results match well, confirming that the ultra-thin lamellar Ag layers are continuous. This type of structure will be important for advanced multilayer superlens designs or other plasmonic devices such as the far-field hyperlens.

The complex permittivity of continuous or nearly-continuous Ag films with thicknesses well above the percolation threshold (5.5-8.5 nm) have also been retrieved and compared with the commonly accepted Johnson & Christy results for bulk silver [18, 19, 32, 33], as shown in

#120778 - $15.00 USD Received 1 Dec 2009; revised 24 Dec 2009; accepted 5 Jan 2010; published 25 Feb 2010

Fig. 7. The ultra-thin continuous Ag films show a quantum size effect [19, 34, 35] as evidenced by increased loss in the fitted model parameters compared to those of bulk silver. It is clear from the retrieved permittivity curves that the thin Ag films show a larger damping rate γ_p and a larger imaginary part of permittivity, particularly at longer wavelengths, than those of bulk Ag films or films modeled using the Drude-Lorentz formalism.

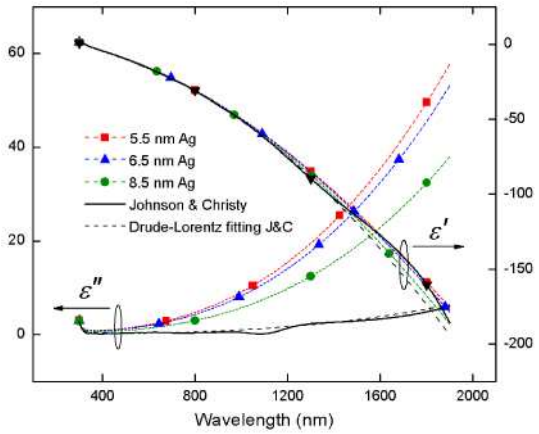

Fig. 7. Comparison of retrieved complex permittivity curves from samples with Ge wetting layers and those of bulk Ag and a fitted Drude-Lorentz model.

The quantum size effect could be described by a mean-free-path-effect model [19, 34, 35]. When the sizes of metal structures such as nanoparticles and grains are smaller than the mean free path of the electrons, the electrons experience collisions with the metal boundaries. These collisions result in an increase in the damping rate and increased loss. Hence, an additional size-dependent term should be included in the damping rate [19, 34, 35]:

$$\gamma_p = \gamma_\infty + A_0 \frac{\upsilon_F}{r}, \tag{2}$$

where γ_∞ is assumed to be a constant for bulk metals, υ_F is the Fermi velocity of Ag, r is the metal particle radius, and the A_0 parameter is a constant around one and depends on the details of the scattering process. Note that in Eq. (2) γ_∞ is in units of s^{-1} and A_0 is dimensionless; for convenience γ_∞ is often specified in eV in the literature. Therefore, Eq. (2) indicates that when the film becomes extremely thin (< 30 nm), the damping rate γ_p is no longer a constant but depends on the particle radius r which is in turn related to the film thickness and grain sizes for amorphous or polycrystalline films) and the A_0-parameter [34]. According to Eq. (2), a thinner film and/or a film with smaller grains will have a larger size-dependent term, resulting in a larger damping rate γ_p. In real applications of ultra-thin continuous Ag films with a Ge sublayer, there should be a balance between the thickness of the film and the tolerable loss in the film.

4. Rapid post-annealing treatment

In order to reduce the loss in our ultra-thin Ag films, a rapid post-annealing treatment was explored for the samples. Our experiments show that a 1-5 minute, 200°C-300°C annealing treatment can significantly reduce the loss of ultra-thin Ag films. The annealing treatment can reduce the loss by allowing grains in polycrystalline or amorphous Ag films to grow in size, thereby reducing the size-dependent term in the damping rate that arises as a result of electron scattering at grain boundaries. This beneficial result of annealing must be carefully controlled to ensure that the Ag film does not change into a semicontinuous, island-like film, which can occur for annealing temperatures that are too high (> 350 °C) or annealing times that are too long (> 6 minutes). It is also critical that the annealing procedure not adversely affect the

#120778 - $15.00 USD Received 1 Dec 2009; revised 24 Dec 2009; accepted 5 Jan 2010; published 25 Feb 2010

roughness of the films. To study this aspect, we measured and compared the RMS roughness from a group of films at different thicknesses before and after annealing. We found that, at the optimized annealing conditions, the RMS roughness values do not significantly change and are still in the range of 0.3-0.7 nm after annealing.

Representative and optimized annealing results for ultra-thin Ag films are shown here. Figure 8 shows the retrieved imaginary permittivity (ε'') values of 10-nm Ag films on a 1-nm Ge wetting layer before and after 3 minutes of annealing at different temperatures. At the same annealing time (3 minutes) and within the proper annealing temperature range, a higher annealing temperature will provide better loss-reducing effect. Annealing the 10-nm Ag film at the optimized condition (3 minutes at 280°C) reduces the damping rate (γ_p) from 0.15 eV to 0.045 eV and reduces the ε'' values by up to 70% within the measured wavelength range.

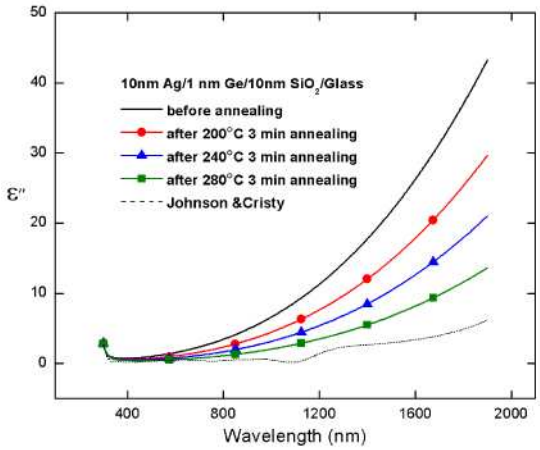

Fig. 8. Comparison of retrieved imaginary part of permittivity (ε'') curves of 10-nm Ag films on a 1-nm Ge wetting layer before and after annealing.

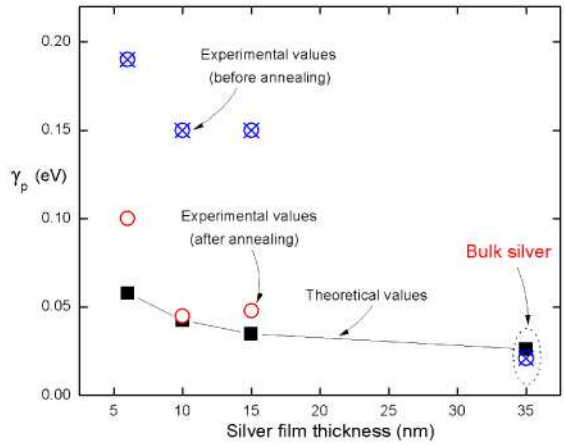

Fig. 9. Theoretically calculated and experimentally retrieved damping rates (γ_p) of Ag films at different thicknesses on a 1-nm Ge wetting layer. Theoretical results were calculated through Eq. (2) with $A_0 = 0.25$.

The theoretical damping rate value of a 10-nm Ag film can be calculated using Eq. (2). The grain size was assumed to be r = 10 nm (which is close to the film thickness) for an ideal condition and the values $\gamma_\infty = 0.0196$ eV (2.98×10^{13} s^{-1}), $A_0 = 0.25$, $\upsilon_F = 1.39\times10^6$ m/s were obtained from Ref [34]. This results in a damping rate of $\gamma_p = 0.0425$ eV, which matches the

#120778 - $15.00 USD Received 1 Dec 2009; revised 24 Dec 2009; accepted 5 Jan 2010; published 25 Feb 2010

retrieved value of γ_p = 0.045 eV obtained from our experiments. Additional calculated and experimentally retrieved damping rates are shown in Fig. 9, indicating that the ultra-thin Ag films have lager loss due to smaller grain sizes. After annealing, the metal grains grow in size and the loss in the film is significantly reduced. Similar loss-reducing effects were also observed for silver-silica lamellar composite films. Therefore, we concluded that this rapid post-annealing treatment is capable of lowering the loss in our ultra-thin Ag films and in silver-silica lamellar composite films to the ideal values allowed by the quantum size effect for smaller grains. It is important to note that this loss reduction is accomplished without degrading the overall film roughness.

5. Conclusion

In summary, we have performed experiments and simulations on the fabrication and characterization of ultra-thin Ag films deposited on a very thin Ge wetting layer. The inclusion of the thin Ge layer as a wetting material acts to drastically reduce the percolation threshold of Ag films. The percolation threshold shifts from a Ag layer thickness of about 11 nm (for Ag deposited on SiO_2 via e-beam evaporation) to a thickness of about 3 nm when a Ge sublayer is included in the fabrication. Hence with a Ge wetting layer it is possible to make ultra-thin, uniformly continuous Ag films at thicknesses of 5.5 nm or larger. In additional experiments, we have confirmed that the addition of a Ge wetting layer reduces the measured surface roughness of continuous Ag films and $(Ag/Ge/SiO_2)_n$ lamellar composite films to around 0.2-0.7 nm. However, the ultra-thin, ultra-smooth Ag films exhibit higher loss than bulk silver due the quantum size effect. For the purpose of reducing the loss of the ultra-thin Ag films, a rapid post-annealing treatment was introduced in our experiments. Our experimental results show that under optimized annealing conditions, the loss of a 10-nm-thick Ag film can be reduced by up to 70% while maintaining low surface roughness in the sample. The rapid post-annealing treatment is able to reduce the loss of the Ag films and silver-silica lamellar composite films to the ideal values allowed by the quantum size effect in small grains, and no further improvement could be expected. Overall, our results indicate that ultra-thin, ultra-smooth and low-loss Ag films and silver-silica lamellar composite films can be achieved by introducing a very thin Ge wetting layer and a rapid post-annealing treatment. This achievement satisfies the demands for both the current superlens and proposed hyperlens designs for high resolution, sub-wavelength imaging.

Acknowledgments

The authors thank Dr. Vladimir Drachev for valuable discussions. We would like to acknowledge constructive improvements suggested by an anonymous reviewer. This work was partially supported by ARO-MURI awards under Grant No. 50342-PH-MUR and W911NF-09-1-0539.

#120778 - $15.00 USD Received 1 Dec 2009; revised 24 Dec 2009; accepted 5 Jan 2010; published 25 Feb 2010